Processing of Polyamide 11 with Supercritical Carbon Dioxide

Jérôme D. Martinache,[†] Joseph R. Royer,[†] Srinivas Siripurapu,[†] Florence E. Hénon,[‡,§] Jan Genzer,[†] Saad A. Khan,[†] and Ruben G. Carbonell*[,†]

Department of Chemical Engineering, North Carolina State University, Raleigh, North Carolina, 27695-7905, and Atofina Chemicals, Inc., King of Prussia, Pennsylvania, 19406-0936

The supercritical carbon dioxide induced swelling and plasticization of polyamide 11 were investigated. The swelling kinetics exhibit an initial region of large swelling, in which the diffusion of CO_2 into the polymer follows Fickian behavior, and a subsequent region of small volume increase that asymptotically approaches an equilibrium swelling value. The diffusion coefficient of CO_2 in polyamide 11 was calculated from the initial slope of the swelling kinetics data. CO_2, injected up to 3 wt % using an extrusion rheometer, is shown to be an effective plasticizer for polyamide 11, lowering the viscosity of the polymer melt by as much as 50%. The use of CO_2 as a blowing agent was also investigated, and we report preliminary foaming attempts using a batch process. We obtained homogeneously distributed foams, featuring well-defined closed cells with an average diameter of 30 μm that had an unfoamed skin layer.

Introduction

The use of supercritical CO_2 ($scCO_2$), among with other supercritical fluids (SCFs), in polymer processing has become of strategic importance in polymer science over the past decade.[1] The physical properties of SCFs can be tuned by slight adjustments to either the pressure or temperature conditions, allowing for tailored solvent properties.[1] SCFs can provide an alternative and "transient" method of plasticizing a polymer melt during processing as compared to traditional additives, which are often difficult to precisely control, separate, and recover.[2] Additionally, $scCO_2$ is inexpensive and generally more environmentally friendly than traditional polymer additives. A significant amount of research has already been aimed at demonstrating the utility of pressure-tuning $scCO_2$ and its potential in polymer synthesis,[3−6] foaming,[7−9] blending,[10,11] coating,[12,13] and additive impregnation.[14,15] All of these specific processes are based on the ability of $scCO_2$ to swell and plasticize a polymer.

The focus of this study is the polyamide 11 (PA 11 or nylon 11)/$scCO_2$ system. The goal of this work is to better understand the interactions of $scCO_2$ with PA 11 and to evaluate the potential industrial applicability of $scCO_2$ as a transient polymer additive for this material. The terms nylon and polyamide are used interchangeably here; nylon is a generic term for any long-chain synthetic polymeric amide in which recurring amide groups are integral to the main polymer chain.[16,17] A previous study indicates that the solubility of molten nylon 6 (T range = 233−241 °C) in CO_2 is approximately 13−17 wt %.[18] Polymers possessing electron-donating functional groups (e.g., the carbonyl functionality of amide groups) have been shown to exhibit specific interactions with CO_2, most probably of Lewis acid−base nature,[19] with the CO_2 molecule acting as an electron acceptor.[20−22] This suggests that lone electron pairs on the PA 11 carbonyl oxygen can interact with the carbon atom of CO_2.[22] Consequently, as nylons exhibit strong intermolecular and intramolecular hydrogen-bonded networks,[16,23] the lower the amide frequency along the polymer chains, the more accessible the carbonyl groups should be for these interactions. Thus, nylon 11 should be more likely than nylon 6 to interact with CO_2, allowing for higher solubility in CO_2 and enhanced plasticization of the melt by CO_2. To the best of our knowledge, this study represents the first investigation of both CO_2-induced swelling and plasticization of nylon 11 under high-pressure conditions.

In this study, we present experimental findings for three aspects of polymer processing. First, we investigated the ability of $scCO_2$ to swell the PA 11 at elevated pressure and temperature conditions, corresponding to typical processing temperatures. Using these experiments, the effects of temperature and pressure on both polymer swelling and the diffusion coefficient of CO_2 into PA 11 are reported. Second, we used a high-pressure slit-die rheometer to probe the effects of CO_2 addition on the viscosity of PA 11. Third, we report attempts to produce thermoplastic foams with PA 11 using CO_2 as the blowing agent. Using a batch foaming technique,[24−27] the potential of using CO_2 as a blowing agent to produce microcellular polymeric foams is addressed.

Experimental Materials and Procedure

Materials. The polymers used in this study are PA 11 semicrystalline thermoplastics commercially available from Atofina S.A. (Paris, France) under the trade name Rilsan. Two different commercial grades of Rilsan PA 11 were used in this study: BMFO (high-fluidity) for both the swelling and foaming studies and BESNO TL (extrusion-grade, free of plasticizers) for the rheology measurements. All samples were supplied in translucent pellet form and were used as received. Table 1 summarizes the physical properties of the two different

* To whom correspondence should be addressed. Phone: 919-515-5118. Fax: 919-515-5831. E-mail: ruben@ncsu.edu.
[†] North Carolina State University.
[‡] Atofina Chemicals, Inc.
[§] Current address: RF Micro Devices, Greensboro, NC, 27409-9421.

10.1021/ie010410b CCC: $20.00
Published on Web 10/12/2001

Table 1. Physical Properties of Polyamide Samples

sample	ρ (g/cm)^3	T_g (°C)	T_m (°C)	crystallinity (%)	M_w (g/mol)	PDI
BMFO	1.03	42.0 ± 1	190.0 ± 1	25	19 400	2.2
BESNO TL	1.03	42.0 ± 1	190.0 ± 1	25	36 200	2.1
nylon 6	1.084	62.5	228.5	–	–	–

polymeric samples. In Table 1, density and crystallinity were specified by the manufactures. Molecular weight information was determined via size-exclusion chromatography (SEC) using an 80/20 mixture of methylene chloride and dichloroacetic acid as the solvent.[28] Differential scanning calorimetery (DSC) was used to determine T_g and T_m. Preliminary swelling experiments were also performed on nylon 6 (PA 6) supplied by Aldrich and used as received. Its physical properties are also found in Table 1. Finally, liquid carbon dioxide (bone dry grade 2.8; purity > 99.8%) was obtained from National Welders and used as received.

Swelling Experiments. Swelling experiments were performed in a high-pressure view cell, previously built to study PDMS swelling behavior.[29] The inside of the cell is rectangular in shape, with dimensions of 0.635 cm (width), 1.587 cm (depth), and 1.587 cm (height). To the best of our knowledge, swelling investigations of a semicrystalline thermoplastic polymer have never been carried out at such high temperatures ($T \geq T_m \approx 190$ °C). To attain these conditions, it was necessary to adapt the original setup by using a new temperature control unit (Barnant 689-0000; 0.1 °C resolution; ±0.2 °C accuracy at 200 °C) in conjunction with a type-K thermocouple and a heating rope (Omegalux FGR-060) in lieu of a convection oven. Given the high viscosity of nylon 11 melts, an additional cylindrical nonporous quartz cuvette (Ruska Instrument Corp.) was used to hold the sample within the view cell. The cylindrical opening of the cuvette had an inner diameter of 0.592 cm and a height of 1.321 cm. The cuvette not only reduced the amount of sample required, but also limited diffusion and swelling of the material to a single dimension and helped increase the turn-around time between experiments.

All polymer samples were dried at 80 °C in a vacuum oven to remove any trace of humidity or gas that could have been dissolved in the polymer. Approximately 100 mg of nylon 11 was introduced into the quartz cuvette. Once the system reached thermal equilibrium (at the set temperature), high-pressure CO_2 was injected into the cell using a syringe pump (Isco 260 D). Figure 1 displays the inside of the cell during a swelling experiment with PA 11. A digital camera was used in conjunction with a public-domain NIH imaging program (developed at the U.S. National Institutes of Health and available at http://rsb.info.nih.gov/nih-image/ or http://www.scioncorp.com/) to capture frames at constant time intervals. Images were collected until no further swelling was detected (typically ~20 h), thus ensuring that equilibrium had been attained. The imaging software was used to correlate the number of pixels to the height of the polymer layer (the top of the layer is taken at the bottom of the meniscus) for each individual picture. The calibration of the corresponding size of the pixels was done using the actual dimensions of the cell.

Rheological Experiments. The extrusion slit-die rheometer used here is based on the extrusion rheometer designs originally developed by Han and Ma[30−32] and later used by Lee et al.[33] Its design is detailed and fully discussed elsewhere,[34] and a schematic diagram of the device is displayed in Figure 2. The base component of the rheometer is a single-screw extruder with an extended 30:1 barrel. Along the length of the barrel, four band heaters are used to establish four individual temperature zones. The final zone is set to the desired measurement temperature, and the other three are incrementally decreased by 5−10 °C at each zone. An injection port for CO_2 is located in the extruder barrel at approximately 70% of the distance from the hopper to the extruder exit. A two-stage screw design is incorporated to help trap the injected CO_2 in the polymer melt and prevent upstream flow of the CO_2. An adapter, a slit die, and a nozzle are attached to the outlet of the extruder. There is a static mixer within the adapter connecting the slit die to the face of the extruder barrel, and the nozzle is required to elevate the pressure within the slit die above the bubble pressure of the polymer/CO_2 mixture, so that a one-phase system is maintained during measurement.

Viscosity calculations on the polymer system were performed using the standard equations for a slit-die rheometer.[35,36] To collect viscosity measurements at constant CO_2 concentrations, a calibration of the mass flow rate was required. This was achieved by feeding PA 11 to the extruder via the hopper and using the extruder screw to generate pressure, thus forcing the melt into the slit die. The pressure drop was recorded, and samples of the melt were taken at the exit of the die to measure the mass flow rate. The volumetric flow rate, which was required to determine the viscosity of the melt, was calculated using the measured mass flow rate and the density estimated from the Sanchez−Lacombe equation of state.[37−39] A list of the Sanchez−Lacombe parameters used for both PA 11 and CO_2 is found in Table 2. The procedure was repeated at different screw rotation rates to develop a viscosity curve and to obtain a mass flow rate calibration as a function of shear rate for the neat polymer. The viscosity of the plasticized melt with dissolved CO_2 was measured following a similar procedure. The desired amount of CO_2, determined from the polymer mass flow rate calibration, which was found to be independent of the CO_2 concentration, was injected by varying the tension on a back-pressure relief valve (Gilson 7037) and the flow rate of the syringe pump (Isco 260D). The CO_2/polymer solution density was also determined using the Sanchez−Lacombe equation of state. The viscosity measurements were relatively insensitive to the density prediction based on the Sanchez−Lacombe equation of state. In these experiments, only a small concentration (2−3 wt %) of high-pressure CO_2 was added to the polymeric melt. The change in the system density calculated by the equation of state and by direct addition of the densities for the two pure fluids is only 1−2%, a low level of error that has also been seen by other investigators.[10,40] In general, this error (1−2%) of the volumetric flow rate is less that the error in the accuracy of the pressure transducers (±0.15 MPa), which corresponds to a maximum viscosity error of approximately ±5%.

Foaming Experiments. *Foam Preparation.* A known amount of polymer mass was charged into a foaming vessel (316 SS high-pressure cylindrical view cell). The inside wall of the vessel was initially lubricated with a mold-release agent (polyethylene glycol) to facilitate easier removal of the final expanded product without disrupting the foam morphology and then heated above

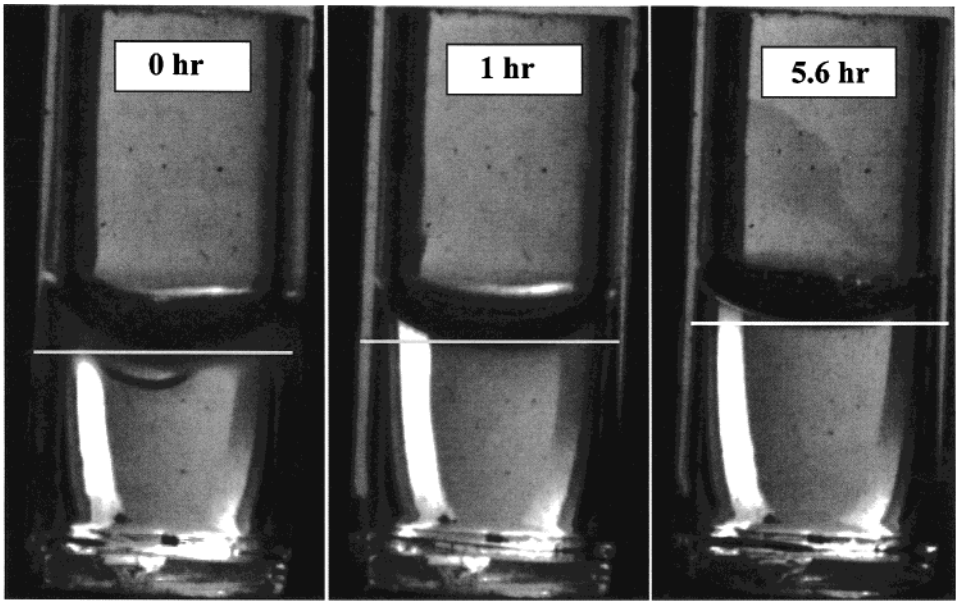

Figure 1. Picture of the PA 11/CO_2 system swelling at 215 °C and 20.6 MPa after 0.0, 1.0, and 5.6 h.

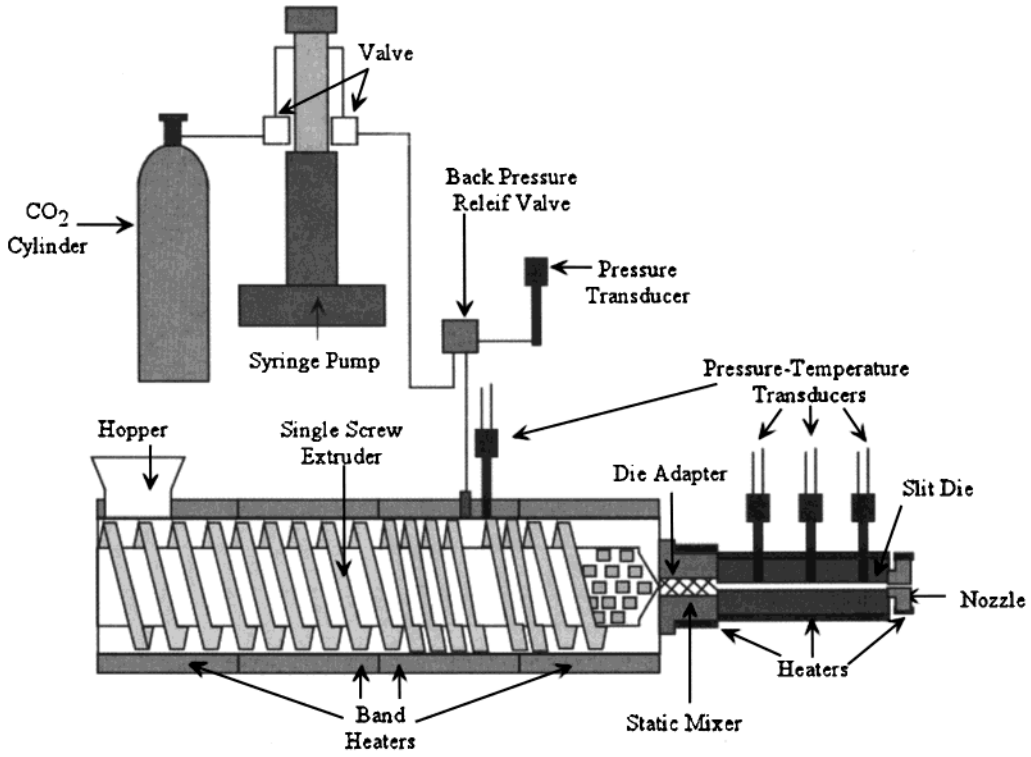

Figure 2. Schematic diagram of high-pressure extrusion slit-die rheometer.

Table 2. Sanchez−Lacombe Pure-Component Characteristic Parameters

material	ρ^* (g/cm^3)	T^* (K)	P^* (MPa)	ref
PA 11[a]	1.035	765.0	465.4	56
CO_2	1.426	328.1	464.2	57

[a] PA 11 data were determined over the temperature range of 478−542 K and the pressure range of 0−50 MPa.

the melting point of the polymer. The vessel was then filled with CO_2 using an Isco pump (Isco 260 D) to a saturation pressure of 34 MPa. When stabilized at the determined temperature, the system was left overnight (∼15 h) to ensure equilibrium absorption of gas by the polymer. Before the pressure was released to foam the polymer, the heating was stopped, and the temperature decreased rapidly to a lower temperature (T_{foam} = 165 °C, P_{foam} = 34.5 MPa) where the system was eventually quenched (over a few seconds) to atmospheric pressure. Microcellular foaming was affected by a pressure-induced phase separation of polymer/gas solution at a fixed temperature.

Foam Characterization. Foams, previously dried under vacuum at 80 °C, were cryofractured after immersion in liquid N_2 and then examined with a Hitachi S3200N by variable-pressure scanning electron microscope (VP-SEM). This particular technique is based on backscattered electron analysis and does not require any kind of conductive coating. It is carried out at an accelerating voltage of 21 kV and a chamber pressure of 70 Pa.

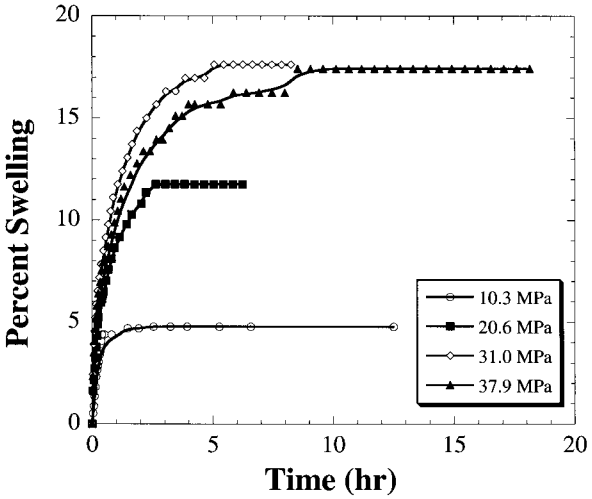

Figure 3. Swelling kinetics of PA 11 at 215 °C at different CO_2 pressures.

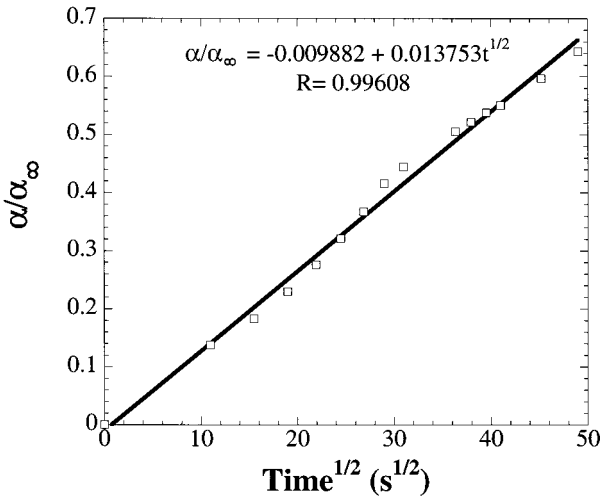

Figure 4. Linear relationship obtained when the initial 60% of the kinetic data are shown as a function of $t^{1/2}$ for PA 11 at 215 °C and 20.6 MPa.

Results and Discussion

Swelling Kinetics. Experimental measurements for PA 11 swelling upon exposure to pressurized carbon dioxide were conducted at 215 °C and at pressures of 10.3, 20.6, 31.0, and 37.9 MPa. To compare the results between pressures, it is convenient to define a parameter for the percent of swelling as seen in eq 1.

$$\text{percent swelling} = \frac{V_t - V_o}{V_o} \tag{1}$$

Here, V_t is the volume of the swollen sample at time t, and V_o is the initial volume of the polymeric sample upon CO_2 pressurization. Using this definition, the percent swelling as a function of time for each of the four different pressures is shown in Figure 3. Replicate experiments were run at 10.3 MPa and the percent difference of the equilibrium percent swelling was found to be less than 5%. Examination of Figure 3 leads to several conclusions. First, the percent swelling of PA 11 increases with increased pressure. Specifically, the percent swelling increases from 4.7 to 17.6 for a pressure increase from 10.3 to 31.0 MPa. However, between 31.0 and 37.9 MPa there appears to be no further increase in the swelling. If we assume that volume and mass uptake are directly related, it is well understood that, as the pressure of CO_2 increases, two competing effects can occur. First, swelling via adsorption and dissolution occurs, and then, in direct contrast, compaction via hydrostatic pressure is observed. It appears that, between 31.0 and 37.9 MPa, a balance between the increase in CO_2 solubility and the compaction by hydrostatic pressure is reached. It is expected that, as the pressure is increased further, the effect of hydrostatic pressure will begin to dominate, and the percent swelling might decrease, as seen with other similar phenomena such as blend miscibility[41,42] and T_g depression.[43,44]

Second, the initial slope of the curve is directly related to the Fickian diffusion coefficient. As expected for Fickian diffusion, the first 60% of the swelling curve data plotted as a function of the square root of time reveals a linear relationship. An example of such a plot is displayed in Figure 4 for the PA 11 system swollen at 215 °C and 37.9 MPa.

Table 3. Data Extracted from PA 11 Swelling Experiments at 215 °C

pressure (MPa)	equilibrium swelling (%)	diffusion coefficient ($cm^2/s \times 10^5$)
10.3	4.7	5.29 ± 0.25
20.6	11.7	5.20
30.1	17.6	2.81
37.9	17.4	2.29

Finally, it appears from qualitative observation that the time required to reach equilibrium swelling of the system increases with pressure. Under 10.3 MPa, the time to attain the equilibrium is approximately 3 h as compared to 10 h under 37.9 MPa. Quantitative values of equilibrium percent swelling can be found in Table 3. Furthermore, some preliminary experiments performed on molten nylon 6 (T = 235 °C) at 20.7 MPa showed a swelling at equilibrium (after 24 h) of only 2.4%, compared to 11.7 for the PA 11 system at 215 °C, thus confirming the assumptions made earlier comparing the increased likelihood of CO_2 interaction with PA 11. Finally, these results demonstrate that CO_2 can be a promising plasticizer for nylon 11.

Diffusion Coefficients of CO_2 into Nylon 11 Melt. The diffusion coefficient (D) of CO_2 into a PA 11 melt can be determined from the initial region of the kinetic swelling data using Fick's second law

$$\frac{\partial c}{\partial t} = \frac{\partial^2 (Dc)}{\partial z^2} \tag{2}$$

where c is the concentration of CO_2 in the polymer melt and z is the direction of diffusion. To solve the above equation, the polymer is assumed to be a semi-infinite medium in the limit of short times. This is a reasonable hypothesis as the polymer is free of CO_2 initially, and it allows for modification of the boundary conditions to establish what amounts to an infinite driving force. It is also valid for up to approximately 60% of the equilibrium swelling for systems that demonstrate Fickian behavior; after the first 60% of the swelling, the shape of the Fickian diffusion profile can become distorted by the changes in the z direction.[45] From the calculations developed previously by others,[29] the following expressions give the mass of penetrant (M_t) taken up into the

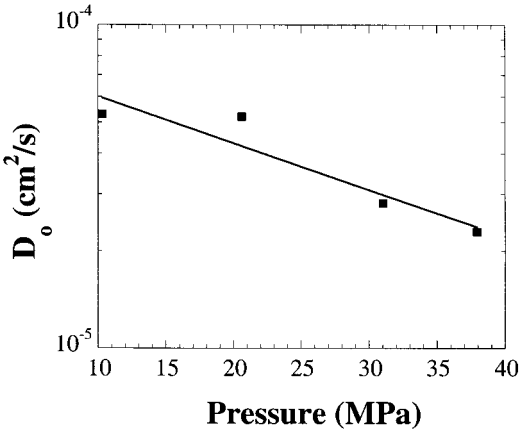

Figure 5. Diffusion coefficients of CO_2 in PA 11 calculated from swelling kinetics at 215 °C as a function of CO_2 pressure.

polymer sample during any elapsed time t and the total mass uptake (M_∞) at equilibrium, respectively

$$M_t = 2\rho_{CO_2} c_\infty \left(\frac{Dt}{\pi}\right)^{1/2} S \tag{3}$$

$$M_\infty = \rho_{CO_2} l_\infty S c_\infty \tag{4}$$

where c_∞ is the CO_2 concentration at equilibrium, l_∞ is the polymer layer thickness at equilibrium, and S is the area of the polymer-free surface.

Assuming that the volume change of mixing is zero, the mass uptake and volume expansion are directly equivalent

$$\frac{\alpha}{\alpha_\infty} \equiv \frac{V_t - V_o}{V_\infty - V_o} = \frac{M_t}{M_\infty} \tag{5}$$

The assumption of no volume change on mixing (ΔV_{mix}) has been shown to be valid for other polymeric systems using this same experimental setup.[29] Additionally Gerhardt et al.[46,47] have shown for PDMS samples that the mixing is more ideal away from the critical point of CO_2. Because these experiments were conducted nearly 200 °C above the critical point, the assumption of ideal mixing is expected to be valid. Using the Sanchez−Lacombe equation of state, we find that, under all experimental conditions, the calculated ΔV_{mix} is less than 3%. This is of the same order of magnitude as the error in the experimental measurements. As a result, eqs 3−5 can be combined to relate the swelling to the diffusion coefficient

$$\frac{\alpha}{\alpha_\infty} = \frac{2}{l_\infty}\left(\frac{Dt}{\pi}\right) \tag{6}$$

This expression can be fitted to the initial part of the swelling kinetics curve plotted as a function of $t^{1/2}$, as shown in Figure 4, to determine a diffusion coefficient for CO_2 in the nylon 11 melt. The diffusion coefficients as a function of operating pressure are displayed in Figure 5 and can also be found in Table 3. Given the enhanced mobility of the molten polymer chains, the value we obtained is consistent with the data found in the literature for diffusion in the solid state, which are 1.91×10^{-8} cm^2/s at 40 °C and 6.33×10^{-8} cm^2/s at 60 °C.[53] Furthermore, the diffusion coefficient value does seem to be slightly dependent on pressure. As the pressure is increased from 10.3 to 37.9 MPa, the diffusion coefficient decreases from 5.293×10^{-5} to 2.294×10^{-5} cm^2/s. This decrease is consistent with the expected compaction or compression of the viscous polymer layer, becoming more pronounced as the operating pressure increases. However, this is not expected to be of major significance because, under our operating conditions, pure-polymer pressure−volume−temperature (PVT) data show that density changes in the PA 11/CO_2 melt phase should be less than 2%.[54]

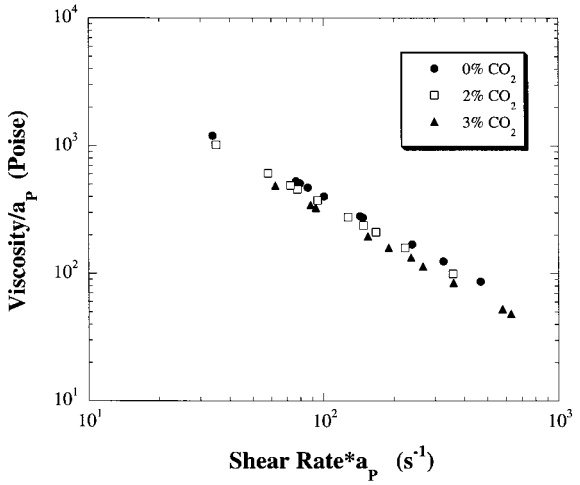

Figure 6. Viscosity measurements for a PA 11 extrusion-grade sample at 225 °C at various CO_2 concentrations and corrected to atmospheric pressure.

Viscosity Reduction With CO_2. Measurements of the viscosity of the PA 11/CO_2 system were performed using the high-pressure extrusion slit-die rheometer at 225 °C. To obtain accurate rheological data for this system, the nylon samples had to be treated with care. First, nylons require adequate drying to handle their high-sensitivity to moisture, causing either hydrolysis (if the moisture level is too high) or post-polymerization (if the moisture level is too low), which can dramatically reduce or increase both the molecular weight and the viscosity of the resin.[16,17] To operate at the same moisture level, all polymer samples were initially dried at 80 °C in a vacuum oven. However, our laboratory extruder was not equipped to control the moisture level during experiments. Furthermore, the characteristics of the screw that we used are themselves not optimized for extrusion of nylons. In particular, the compression ratio along the metering zone is only 2:1, because of the decompression zone required to inject CO_2, although nylons usually require a value between 3:1 and 3.5:1 to overcome significant shrink rates under extrusion conditions.[16,17] The poor screw optimization requires that the flow rate of nylon in the extrusion system be closely monitored. Operating under these special parameters, it is possible to obtain accurate viscosity data for the PA 11/CO_2 system.

Figure 6 displays the viscosity for a PA 11 extrusion-grade sample plotted against shear rate at 225 °C with CO_2 concentrations of 0, 2, and 3%. To obtain viscosity measurements from the slit-die rheometer several corrections to the data must be applied. Because the slit-die instrument is a pressure-driven rheometric device, the pressure of each of the experimental points varies with viscosity, screw rotation rate, nozzle size, and CO_2 injection pressure. A pressure correction developed in previous work for polymeric melts well above T_g was used with these data.[48] The pressure correction based

on an Arrhenius model of visocelastic scale is[48]

$$\ln a_P = \ln\left(\frac{\eta_{T_g,P_o,mix}}{\eta_{T_g,P,mix}}\right) = \left[\frac{E_a}{R}\left(\frac{1}{T_{g_{mix}},P_o} - \frac{1}{T_{g_{mix},P}}\right)\right] \quad (7)$$

Here, a_P is the viscoelastic pressure shift factor; P and P_o are the experimental and atmospheric pressures, respectively; E_a is the activation energy of viscous flow; and T_{gmix} is the glass transition temperature for the PA 11/CO_2 mixture calculated via the Chow model.[49] The activation energy of viscous flow, E_a, was estimated using a technique developed by Porter et al.[50] with a value of 10×10^{-5} K^{-1} for the thermal expansion coefficient.[51] In addition to the pressure correction, the apparent viscosity data were corrected to reflect the actual viscosity using the Rabinowitsch−Weissenberg correction for the slit-die geometry.[52] Examination of Figure 5 reveals that CO_2 addition to the PA 11 melt greatly reduces the system viscosity. Specifically, the 2 and 3 wt % additions of CO_2 reduce the viscosity of the PA 11 melt by 12.5 and 25%, respectively. This significant shift in viscosity confirms that CO_2 acts as an efficient plasticizer for PA 11. This result is of the same order of magnitude as observed for polystyrene,[35] which has a much stronger affinity for CO_2.

Foaming Attempt. Most studies on microcellular foaming in the past have been done with amorphous polymers such as polystyrene.[55] Classical nucleation theory has been shown to describe microcellular foaming of poly(methyl methacrylate)[25] and is widely accepted now as the foaming mechanism. Cooling the polymer melt to a temperature closer to its glass transition temperature has been shown to increase cell nucleation density. As suggested by Behravesh et al.,[55] the cell wall stability can be improved by increasing the so-called melt strength. By definition, the melt strength is the degree of resistance of the extensional flow of the cell wall during the drainage of polymer in the cell wall when volume expansion takes place. Consequently, cell coalescence tends to be suppressed, and smaller cell nuclei are frozen in with decreased foaming temperature.

During the saturation step of the temperature program, the polymer is maintained in its molten state ($T \geq 190$ °C). By doing so, we increase the polymer chain mobility, which facilitates penetration and diffusion of the CO_2 molecules into the matrix. This also ensures formation of a homogeneous polymer/CO_2 solution. Because polyamide 11 has a crystalline melting point ($T_m = 190$ °C) apart from its glass transition temperature ($T_g = 42$ °C), the foaming temperature was set as close as possible to the melting point of the polymer melt swollen with carbon dioxide. Before initiating the foaming process by quenching the system from 34 MPa down to atmospheric pressure over a few seconds, we let the melt cool to the desired foaming temperature ($T_{foam} = 165$ °C). As the foaming vessel is equipped with sapphire windows, we found visually that lower temperatures led to phase separation of the polymer/gas solution through the appearance of opaque crystallites in the transparent melt. A micrograph of a PA 11 foam sample is shown in Figure 7. The foam obtained, featuring well-distributed spherical closed cells, is homogeneous and has an an unfoamed skin layer. The resulting foam has the same degree of crystallinity as the unfoamed polymer. The number of cells seen in the picture was counted, and the cell density of the foam was calculated, using

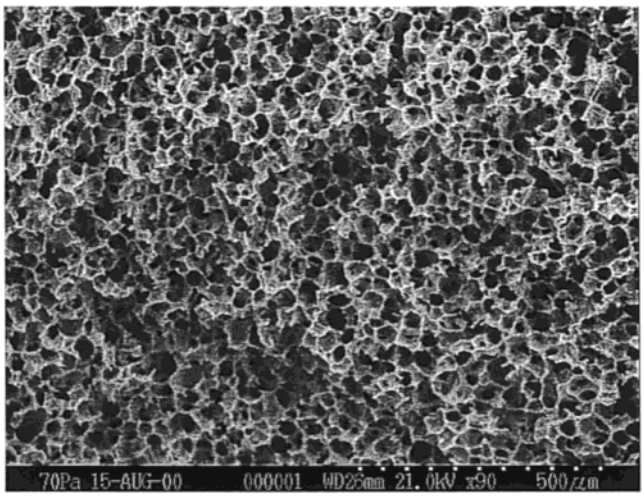

Figure 7. VP-SEM micrograph of a PA 11 foam sample (saturation time = 15 h, saturation pressure = 34.5 MPa, saturation temperature = 190 °C, nucleation temperature = 165 °C).

the method described by Kumar and Suh.[38] The number of bubbles nucleated per cubic centimeter (N_f) can be expressed as

$$N_f = \left(\frac{nM^2}{A}\right)^{3/2} \quad (8)$$

where A is the area of the micrograph, M is the magnification factor, and n is the number of bubbles seen in the micrograph. The bulk density of the foam was determined by immersing a sample in water and measuring the mass of the liquid volume displaced, in accordance with Archimedes' principle.

This foam exhibits an average cell diameter of ∼30 μm, a cell density of 1.2×10^7 cells/cm^3, and a bulk density of 0.29 g/cm^3, parameters that are comparable to those of a typical microcellular polymeric foam (MPF). A typical MPF structure has a uniform distribution of closed cells with a mean cell diameter of 10 μm (or less) and a cell density of 10^8 cells/cm^3 (or more).[40] Our results are very encouraging given the processing problems associated with the foaming of nylon 11, including its degree of crystallinity (∼25%) and the large difference between the melting and glass transition temperatures ($T_m - T_g \approx 150$ °C). This latter quality prevents the nucleation step from being conducted near the T_g of the melt, which is an important factor in reducing cell coalescence. The most simple and economically sound way to improve the quality of our foams, and to tend toward the MPF parameters, would be to operate at lower temperature, which would enhance the melt strength, as discussed previously, and decrease CO_2 diffusion in the system when nucleation occurs. However, lower temperatures induce phase separation of the polymer/gas solution. A detailed study of the effects of the foaming pressure and control of the pressure drop rate might lead to improved MPF morphologies.

Conclusion

Several properties of the PA 11/scCO_2 system were investigated. Characteristics of the swelling kinetics of molten PA 11 in CO_2 were determined, and diffusion coefficients of CO_2 into the polymer melts were calculated at 215 °C. We found that the diffusion of CO_2 into

PA 11 melts exhibits Fickian behavior until two-thirds of the equilibrium swelling value is reached. The CO_2 pressure was shown to have a dramatic impact on the equilibrium swelling value and the time required to reach the equilibrium, as well as to slightly decrease the diffusion itself. CO_2 was also shown to be an effective plasticizer for PA 11, lowering the viscosity of the polymer melt by as much as 25% at 225 °C. Finally, the preliminary foaming attempt was successful, resulting in a homogeneous foam featuring well-distributed spherical closed cells with an average diameter of about 30 μm. The results gathered in this paper demonstrate the potential of PA 11 for CO_2-assisted processes currently under development.

Nomenclature

A = area of the micrograph (cm^2)
a_P = pressure shift factor
c = penetrant concentration (g/g)
c_∞ = CO_2 concentration at equilibrium (g/g)
D = diffusion coefficient (cm^2/s)
E_a = activation energy of viscous flow (J/mol)
l_∞ = height of the polymer layer at equilibrium (cm)
M = magnification factor
M_t, M_∞ = masses of penetrant taken up into the polymer at any time t and at equilibrium, respectively (g)
n = number of bubbles seen in the micrograph
N_f = number of bubbles nucleated per cubic centimeter (cm^{-3})
P, P_o, P_{foam}= pressure, atmospheric pressure, and foaming pressure, respectively (MPa)
R = ideal gas constant [J/(mol K)]
S = area of the polymer-free surface (cm^2)
T_g, T_m, T_{foam}= glass transition temperature, melting temperature, and foaming temperature, respectively (K)
t = time (s)
V_o, V_t, V_∞ = volume of the polymer layer initially, at any time t, and at equilibrium, respectively (cm^3)
ΔV_{mix} = change of volume upon mixing (cm^3)
z = axial coordinate (cm)
α, α_∞ = degrees of swelling at any time t and at equilibrium, respectively
ρ_{CO_2} = density of CO_2 under the operating conditions (g/cm^3)
η = melt viscosity (P)

Acknowledgment

The authors acknowledge partial support from the Kenan Center for the Utilization of Carbon Dioxide in Manufacturing and the STC Program of the National Science Foundation under Agreement CHE-9876674. In addition, we would like to acknowledge Atofina Chemicals, Inc. (King of Prussia, PA), for donation of the polymers, DSC and GPC analysis, and funding. J.D.M. also thanks Atofina, S.A., for financial support.

Literature Cited

(1) Shine, A. D. In *Physical Properties of Polymer Handbook*; Mark, J. E., Ed.; AIP Press: New York, 1996; pp 249−256.
(2) Combey, M. *Plasticisers, Stabilisers, and Fillers*; Iliffe Books Ltd: London, 1972.
(3) DeSimone, J. M.; Guan, Z.; Eisbernd, C. S. *Science* **1992**, *257*, 945−947.
(4) DeSimone, J. M.; Maury, E. E.; Menceloglu, Y. Z.; McClain, J. B.; Romack, T. J.; Combes, J. R. *Science* **1994**, *265*, 356−359.
(5) Shaffer, K. A.; DeSimone, J. M. *Trends Polym. Sci.* **1995**, *3*, 146−153.
(6) McClain, J. B.; Betts, D. E.; Canelas, D. A.; Samulski, E. T.; DeSimone, J. M.; Londono, J. D.; Wignall, G. D. *Science* **1996**, *274*, 2049−2052.
(7) Goel, S. K.; Beckman, E. J. *AIChE J.* **1995**, *41*, 357−367.
(8) Doroudiani, S.; Park, C. B.; Kortschot, M. T. *Polym. Eng. Sci.* **1998**, *38*, 1205−1215.
(9) Park, C. B.; Behravesh, A. H.; Venter, R. D. *Polym. Eng. Sci.* **1998**, *38*, 1812−1823.
(10) Elkovitch, M. D.; Lee, L. J.; Tomasko, D. L. *Polym. Eng. Sci.* **2000**, *40*, 1850−1861.
(11) Lee, M.; Tzoganakis, C.; Park, C. B. *Polym. Eng. Sci.* **1998**, *38*, 1112−1120.
(12) Shim, J.; Yates, M. Z.; Johnston, K. P. *Ind. Eng. Chem. Res.* **1999**, *38*, 3655−3662.
(13) Tsutsumi, A.; Nakamoto, S.; Mineo, T.; Yoshida, K. *Powder Technol.* **1995**, *85*, 275−278.
(14) Berens, A. R.; Huvard, G. S.; Korsmeyer, R. W.; Kunig, F. W. *J. Appl. Polym. Sci.* **1992**, *46*, 231−242.
(15) Li, D.; Han, B. *Ind. Eng. Chem. Res.* **2000**, *39*, 4506−4509.
(16) Kohan, M. I. In *Nylon Plastics*; Wiley & Sons: I., Ed.: New York, 1973; pp 14−29.
(17) Simonds, H. R.; Church, J. M. In *A Concise Guide to Plastics*; Corp., R. P., Ed.: New York, 1963; pp 37−39.
(18) Bangert, L. H.; Lundberg, J. L.; Muzzy, J. D.; Hoyas, G. H.; Olson, L. H. *Advanced Technology Applications in Garment Processing*; Georgia Institute of Technology: Atlanta, GA, 1977.
(19) Hyatt, J. A. *J. Org. Chem.* **1984**, *49*, 5097−5101.
(20) Hildebrand, J. H.; Prausnitz, J. M.; Scott, R. L. *Regular and Related Solutions: The Solubility of Gases, Liquids and Solids*; Van Nostrand Reinhold: New York, 1970; p 228.
(21) Sigman, M. E.; Lindley, S. M.; Leffler, J. E. *J. Am. Chem. Soc.* **1985**, *107*, 1471−1472.
(22) Kazarian, S. G.; Vincent, M. F.; Bright, F. V.; Liotta, C. L.; Eckert, C. A. *J. Am. Chem. Soc.* **1996**, *118*, 1729−1736.
(23) Suresh, S. J.; Enick, R. M.; Beckman, E. J. *Macromolecules* **1994**, *27*, 348−356.
(24) Kumar, V.; Suh, N. P. *Polym. Eng. Sci.* **1990**, *30*, 1323−1329.
(25) Goel, S. K.; Beckman, E. J. *Polym. Eng. Sci.* **1994**, *34*, 1137−1147.
(26) Liang, M. T.; Wang, C. M. *Ind. Eng. Chem. Res.* **2000**, *39*, 4622−4626.
(27) Stafford, C. M.; Russell, T. P.; McCarthy, T. J. *Macromolecules* **1999**, *32*, 7610−7616.
(28) Mourey, T. H.; Bryan, T. G. *J. Chromatogr. A* **1994**, *679*, 201−205.
(29) Royer, J. R.; DeSimone, J. M.; Khan, S. A. *Macromolecules* **1999**, *32*, 8965−8973.
(30) Han, C. D.; Ma, C. *J. Appl. Polym. Sci.* **1983**, *28*, 831−850.
(31) Han, C. D.; Ma, C.-Y. *J. Appl. Polym. Sci.* **1983**, *28*, 851−860.
(32) Ma, C.-Y.; Han, C. D. *J. Cell. Plast.* **1982**, 361−370.
(33) Lee, M.; Park, C. B.; Tzoganakis, C. *Polym. Eng. Sci.* **1999**, *39*, 99−109.
(34) Royer, J. R.; Gay, Y. J.; DeSimone, J. M.; Khan, S. A. *J. Polym. Sci. B: Polym. Phys.* **2000**, *38*, 3168−3180.
(35) Wales, J. L. S.; denOtter, J. L.; Janeschitz-Kriegl, H. *Rheol. Acta* **1965**, *4*, 146−152.
(36) Macosko, C. W. *Rheology: Principles, Measurements, and Applications*; VCH Publishers: New York, 1993.
(37) Lacombe, R. H.; Sanchez, I. C. *J. Phys. Chem.* **1976**, *80*, 2568−2580.
(38) Sanchez, I. C. *Macromolecules* **1978**, *11*, 1145−1156.
(39) Sanchez, I. C.; Lacombe, R. H. *J. Phys. Chem.* **1976**, *80*, 2352−2362.
(40) Kwag, C.; Manke, C. W.; Gulari, E. *J. Polym. Sci. B: Polym. Phys.* **1999**, *37*, 2771−2781.
(41) Watkins, J. J.; Brown, G. D.; Pollard, M. A.; Ramachandra-Rao, V.; Russell, T. P. *Macromolecules* **1999**, *32*, 7737−7740.
(42) Walker, T. A.; Raghavan, S. R.; Royer, J. R.; Smith, S. D.; Wignall, G. W.; Melnichenko, Y.; Khan, S. A.; Spontak, R. J. *J. Phys. Chem. B* **1999**, *103*, 5472−5476.
(43) Condo, P. D.; Sanchez, I. C.; Panayiotou, C. G.; Johnston, K. P. *Macromolecules* **1992**, *25*, 6119−6127.
(44) Condo, P. D.; Paul, D. R.; Johnston, K. P. *Macromolecules* **1994**, *27*, 365−371.
(45) Crank, J. *The Mathematics of Diffusion*, 2nd ed.; Clarendon Press: Oxford, U.K., 1975.

(46) Gerhardt, L. J.; Manke, C. W.; Gulari, E. *J. Polym. Sci. B: Polym. Phys.* **1997**, *35*, 523−534.
(47) Gerhardt, L. J.; Garg, A.; Manke, C. W.; Gulari, E. *J. Polym. Sci. B: Polym. Phys.* **1998**, *36*, 1911−1918.
(48) Royer, J. R.; DeSimone, J. M.; Khan, S. A. *J. Polym. Sci. B: Polym. Phys.*, in press.
(49) Chow, T. S. *Macromolecules* **1980**, *13*, 362−364.
(50) Porter, R. S.; Chauh, H. H.; Wang, J. S. *J. Rheol.* **1995**, *39*, 649−654.
(51) Ohkashi, Y. In *Polymeric Materials Encylopedia*; Salamone, J. S., Ed.; CRC Press: Boca Raton, FL, 1996; p 2070.
(52) Laun, H. M. *Rheol. Acta* **1983**, *22*, 171−185.

Received for review May 7, 2001
Revised manuscript received August 23, 2001
Accepted August 27, 2001

IE010410B